

# Simultaneous Measurements of Droplet Size and Transient Temperature Within Surface Water Droplets

Hui Hu\* and De Huang†  
Iowa State University, Ames, Iowa 50011

DOI: 10.2514/1.37158

A lifetime-based molecular tagging thermometry technique was developed for achieving simultaneous measurements of droplet size and transient temperature distribution within a small water droplet over a solid surface. For molecular tagging thermometry measurements, a pulsed laser is used to tag phosphorescent 1-BrNp · Mβ-CD · ROH molecules premixed within a small water droplet. Long-lived laser-induced phosphorescence is imaged at two successive times after the same laser excitation pulse. While the size of the water droplet (in terms of volume, height, contact area, and contact angle of the water droplet) can be determined instantaneously from the acquired phosphorescence images, the transient temperature measurement is achieved by taking advantage of the temperature dependence of phosphorescence lifetime, which is estimated from the intensity ratio of the acquired phosphorescence image pair. The feasibility and implementation of the lifetime-based molecular tagging thermometry technique were demonstrated by conducting simultaneous measurements of droplet size and spatially and temporally resolved temperature distribution inside a convectively-cooled micro-sized water droplet over an aluminum test plate to quantify the unsteady mass and heat transfer processes within the small water droplet to elucidate underlying physics to improve our understanding about microphysical phenomena associated with aircraft icing studies.

## I. Introduction

**A**IRCRAFT icing is widely recognized as a significant hazard to aircraft operations. When an aircraft or rotorcraft flies through a cloud of supercooled water droplets, some of the droplets follow trajectories to allow them to impact and freeze on exposed aircraft surfaces to form ice shapes. Ice may accumulate on every exposed frontal surface of the airplane, not just on the wings, propeller, and windshield but also on the antennas, vents, intakes, and cowlings. Icing accumulation can degrade the aerodynamic performance of an aircraft significantly by increasing drag while decreasing lift [1]. In moderate to severe conditions, an aircraft can become so iced up that continued flight is impossible. The airplane may stall at much higher speeds and lower angles of attack than normal. It can roll or pitch uncontrollably, and recovery may be impossible [2]. Ice can also cause engine stoppage by either icing up the carburetor or, in the case of a fuel-injected engine, blocking the engine's air source.

Advancing the technology for safe and efficient aircraft operation in atmospheric icing conditions requires a better understanding of the microphysical phenomena associated with the accretion and growth of ice and the attendant aerodynamic effects. To elucidate the underlying physics associated with microphysical phenomena for various aircraft icing studies, experimental techniques capable of providing accurate measurements to quantify important ice-growth physical processes such as droplet dynamics, unsteady heat transfer process within water droplets or ice crystals, and phase change process of supercooled water droplets over smooth/rough surfaces, are highly desirable. In the present study, a novel, lifetime-based molecular tagging thermometry (MTT) technique was developed and implemented to achieve simultaneous measurements of droplet size and transient temperature distributions within small water

droplets to quantify unsteady mass and heat transfer processes within small convectively cooled water droplets over solid surfaces in order to elucidate underlying physics to improve our understanding about microphysical phenomena associated with aircraft icing studies.

The research work described in the present study can be considered as an extension of the recent work of Hu and Koochesfahani [3], who invented a molecular tagging velocimetry and thermometry technique for the simultaneous measurements of fluid velocity and temperature distributions in liquids. In the sections that follow, the technical basis of the lifetime-based MTT will be described briefly along with the related properties of the phosphorescent tracer to be used for the MTT measurements. The application of the lifetime-based MTT technique to conduct simultaneous measurements of droplet size and spatially and temporally resolved temperature distribution within a convectively cooled, micro-sized water droplet over an aluminum test plate will be given to quantify the unsteady mass and heat transfer processes within the small water droplet to demonstrate the feasibility and implementation of the lifetime-based MTT technique.

## II. Lifetime-Based Molecular Tagging Thermometry Technique

It is well known that both fluorescence and phosphorescence are molecular photoluminescence phenomena [4]. Compared with fluorescence, which typically has a lifetime on the order of nanoseconds, phosphorescence can last as long as microseconds, even minutes. Because emission intensity of photoluminescence is a function of the temperature for some substances, both fluorescence and phosphorescence of tracer molecules may be used for temperature measurements.

According to Beer's Law for low concentration of the tracer molecules and unsaturated laser excitation [4], photoluminescence intensity  $I_p$  (both fluorescence and phosphorescence) can be expressed by following equation:

$$I_p = AI_i C \varepsilon \Phi \quad (1)$$

where  $I_i$  is the local incident laser intensity,  $C$  the concentration of tracer molecules,  $\varepsilon$  the absorption coefficient, and  $\Phi$  the quantum efficiency.  $A$  is the fraction of the photoluminescence emission collected by a CCD (charge-coupled device) detector.

Presented as Paper 0265 at the 46th AIAA Aerospace Sciences Meeting and Exhibit, Reno, NV, 7–10 January 2008; received 14 February 2008; accepted for publication 28 August 2008. Copyright © 2008 by Hui Hu and De Huang. Published by the American Institute of Aeronautics and Astronautics, Inc., with permission. Copies of this paper may be made for personal or internal use, on condition that the copier pay the \$10.00 per-copy fee to the Copyright Clearance Center, Inc., 222 Rosewood Drive, Danvers, MA 01923; include the code 0001-1452/09 \$10.00 in correspondence with the CCC.

\*Assistant Professor, Department of Aerospace Engineering; huhui@iastate.edu, Senior Member AIAA.

†Graduate Student, Department of Aerospace Engineering.

### A. Laser-Induced-Fluorescence-Based Techniques for Droplet Temperature Measurements

Laser-induced fluorescence (LIF) techniques have been widely used for temperature measurements of liquid droplets for combustion applications [5,6]. Harris et al. [7] used a LIF-based technique to conduct quantitative measurements of internal circulation in droplets. For some fluorescent molecules, such as Rhodamine B, the absorption coefficient and quantum efficiency are temperature dependent. Therefore, in principle, fluorescence intensity may be considered to depend only on temperature as long as the incident laser excitation is uniform and the concentration of the tracer molecules remains constant in the measurement region. In practice, however, it is very difficult, if not impossible, to ensure a temporally and spatially nonvarying incident laser excitation and/or uniform molecular tracer concentration in the measurement region for heat transfer studies due to the temperature dependence of the index of refraction for the work fluid. The issue could become much more serious for the transient temperature measurements within small water droplets over solid surfaces because the curved droplet surfaces would cause tremendous variation of laser illumination (i.e., refraction, reflection, and scattering) in the measurement domain. The photobleaching effect may also become significant due to the small size of the water droplets. Such issues may cause significant errors in the droplet temperature measurement.

To decouple the effects of the nonuniformity of incident laser illumination and the molecular tracer concentration (due to photobleaching) on fluid temperature measurement, several ratiometric LIF techniques have been developed recently [5,6,8–11]. The ratiometric LIF techniques developed for the temperature measurement of liquid droplets are usually called two-color LIF techniques [10,11]. The two-color LIF technique achieves temperature measurements by taking advantage of the differences in temperature sensitivity of fluorescence emission at two different bands of the same fluorescent dye. After taking the ratio of the fluorescence emission intensity simultaneously collected at two different emission bands (i.e., two colors), the effects of the nonuniformity of incident laser illumination and concentration of the fluorescent tracer molecules on the droplet temperature measurements can be eliminated.

It should be noted that it usually requires two cameras with various mirrors, optical filters, and lenses in order to capture two fluorescence images at the same time to implement the two-color LIF method. It also requires a careful image registration or coordinate mapping procedure in order to establish a spatial correlation between the two acquired fluorescence images acquired by two difference cameras for the LIF intensity ratio calculation. The optical distortions due to the different mirrors, filters, and lenses mounted in the fronts of different cameras can cause ambiguities to locate corresponding fluorescent molecules in the two acquired fluorescence images for the LIF intensity ratio calculation. This would result in uncertainties for the droplet temperature measurements.

By using LIF-based thermometry techniques, the total fluorescence intensity (integration of all of the fluorescence emission along a time axis) is usually collected for the temperature measurement due to the short emission lifetime of fluorescence (on the order of nanoseconds). Based on the calibration curves of the collected fluorescence intensity (or intensity ratio) vs temperature, the collected fluorescence intensity (or intensity ratio) distributions are converted to fluid temperature distributions. Therefore, LIF-based techniques are actually *intensity-based* techniques for temperature measurement.

### B. Lifetime-Based Molecular Tagging Thermometry Technique

Laser-induced phosphorescence (LIP) techniques have also been suggested recently to conduct temperature measurements of “in-flight” or levitated liquid droplets [12,13]. Compared with LIF techniques, the relatively long lifetime of phosphorescence could be used to prevent interference from scattered/reflected light and any fluorescence from other substances (such as from solid surfaces) that are present in the measurement area, by simply putting a small time

delay between the laser excitation pulse and the starting time for phosphorescence image acquisitions. Furthermore, LIP was found to be three to four times more sensitive to temperature variation compared with LIF [12–14], which is favorable for the accurate measurements of small temperature differences within small liquid droplets.

The MTT technique described at here is a LIP-based technique, which can be considered as an extension of the molecular tagging velocimetry and thermometry technique developed by Hu and Koochesfahani [3]. Unlike most commonly used LIF-based techniques that rely on information obtained from the *intensity axis* of the *fluorescence* emission process, the lifetime-based MTT technique described in the present study relies on the information contained in the *time axis* of the *phosphorescence* emission process, as temperature change would cause significant variation in the phosphorescence lifetime for some phosphorescent dyes. For MTT measurement, a pulsed laser is used to tag phosphorescent tracer molecules (e.g., phosphorescent dye) premixed in the working fluid. The long-lived LIP emission is imaged at two successive times after the same laser excitation pulse. The LIP emission lifetime distribution can be estimated from the intensity ratio of the acquired phosphorescence image pair. While the size of a small droplet can be determined from the acquired phosphorescence images, the temperature distribution within the small water droplet can be derived by taking advantage of the temperature dependence of phosphorescence lifetime. It should be noted that both the present MTT measurement and the work of Omrane et al. [12,13] are based on a similar idea of achieving temperature measurement by taking advantage of temperature dependence of phosphorescence lifetime. The work of Omrane et al. [12,13] is only a single-point feasibility study using photomultiplier-based instrumentation. The work present at here, to our knowledge, is the first planar temperature field measurement to achieve simultaneous measurements of droplet size and temporally and spatially resolved temperature distribution within a small water droplet based on direct imaging of phosphorescence lifetime with a conventional image-detecting CCD camera.

The technical basis of the lifetime-based MTT measurements is given briefly at here. For dipole allowed radiation, the intensity of phosphorescence emission decays exponentially [4]. As described in Hu et al. [14], for a dilute solution and unsaturated laser excitation, the collected phosphorescence signal  $S$ , by using a gated imaging detector with integration starting at a delay time  $t_o$  after the laser pulse and a gate period of  $\delta t$ , can be given by

$$S = AI_i C \varepsilon \Phi_p (1 - e^{-\delta t/\tau}) e^{-t_o/\tau} \quad (2)$$

where  $A$  is a parameter representing the detection collection efficiency,  $I_i$  is the local incident laser intensity,  $C$  is the concentration of the phosphorescent dye (the tagged molecular tracer),  $\varepsilon$  is the absorption coefficient, and  $\Phi_p$  is the phosphorescence quantum efficiency. The emission lifetime  $\tau$  refers to the time at which the intensity drops to 37% (i.e.,  $1/e$ ) of the initial intensity.

In general, the absorption coefficient  $\varepsilon$ , quantum yield  $\Phi_p$ , and the emission lifetime  $\tau$  are temperature dependent, resulting in a temperature-dependent phosphorescence signal  $S$ . Thus, in principle, the collected phosphorescence signal  $S$  may be used to measure fluid temperature if the incident laser intensity and the concentration of the phosphorescent dye remain constant (or are known) in the region of interest. It should be noted that the collected phosphorescence signal  $S$  is also the function of incident laser intensity  $I_i$  and the concentration of the phosphorescent dye  $C$ . Therefore, the spatial and temporal variations of the incident laser intensity and the nonuniformity of the phosphorescent dye in the region of interest would have to be corrected separately in order to derive quantitative temperature data from the acquired phosphorescence images. To overcome this problem, Hu and Koochesfahani [15] developed a lifetime-based thermometry to eliminate the effects of incident laser intensity and concentration of phosphorescent dye on temperature measurements.

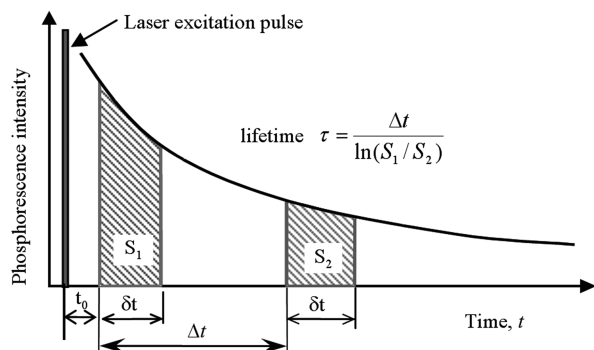


Fig. 1 Timing chart for lifetime-based thermometry technique.

The following information describes how the lifetime-based thermometry works. As illustrated in Fig. 1, the phosphorescence emission of the tagged tracer molecules is interrogated at two successive times after the same laser excitation pulse. The first image is detected at the time  $t = t_0$  after laser excitation for a gate period  $\delta t$  to accumulate the phosphorescence intensity  $S_1$ , whereas the second image is detected at the time  $t = t_0 + \Delta t$  for the same gate period to accumulate the phosphorescence intensity  $S_2$ . It is easily shown, using Eq. (2), that the ratio of the two phosphorescence signals ( $R$ ) is given by

$$R = \frac{S_2}{S_1} = e^{-\Delta t/\tau} \quad (3)$$

In other words, the intensity ratio of the two successive phosphorescence images is only a function of the phosphorescence lifetime  $\tau$  and the time delay  $\Delta t$  between the images, which is a controllable parameter. This ratiometric approach eliminates the variations in the initial intensity and, along with it, any temporal and spatial variations in the incident laser intensity (e.g., reflecting and/or scattering) and nonuniformity of the dye concentration (e.g., due to bleaching). The phosphorescence lifetime can be calculated according to

$$\tau = \frac{\Delta t}{\ln(S_1/S_2)} \quad (4)$$

For a given molecular tracer and fixed  $\Delta t$  value, Eq. (3) defines a unique relation between phosphorescence intensity ratio  $R$  and fluid temperature  $T$ , which can be used for thermometry as long as the temperature dependence of phosphorescence lifetime is known.

### C. Phosphorescent Molecular Tracers Used in the Present Study

The phosphorescent molecular tracer used in the present study is phosphorescent triplex 1-BrNp · Mβ-CD · ROH. The phosphorescent triplex 1-BrNp · Mβ-CD · ROH is actually the mixture compound of three different chemicals, which are lumophore (indicated collectively by 1-BrNp), maltosyl-β-cyclodextrin (indicated collectively by Mβ-CD), and alcohols (indicated collectively by ROH). Further information about the chemical and photoluminescence properties of the phosphorescent triplex is available [16–19]. In the present study, we used a concentration of  $2 \times 10^{-4}$  M for Mβ-CD, a saturated (approximately  $1 \times 10^{-5}$  M where M is the molar concentration) solution of 1-BrNp and a concentration of 0.06 M for the alcohol (ROH), as suggested by Gendrich et al. [18].

Upon the pulsed excitation of a UV laser (quadrupled wavelength of Nd:YAG laser at 266 nm for the present study), the phosphorescence lifetime of the phosphorescent triplex (1-BrNp · Mβ-CD · ROH) molecules in an aqueous solution changes significantly with temperature. Figure 2 shows the measured phosphorescence lifetimes of 1-BrNp · Mβ-CD · ROH molecules as a function of temperature, which were obtained through a calibration experiment similar to those described in Hu and Koochesfahani [3,15]. It can be seen clearly that phosphorescence lifetime of 1-BrNp · Mβ-CD · ROH molecules varies significantly with

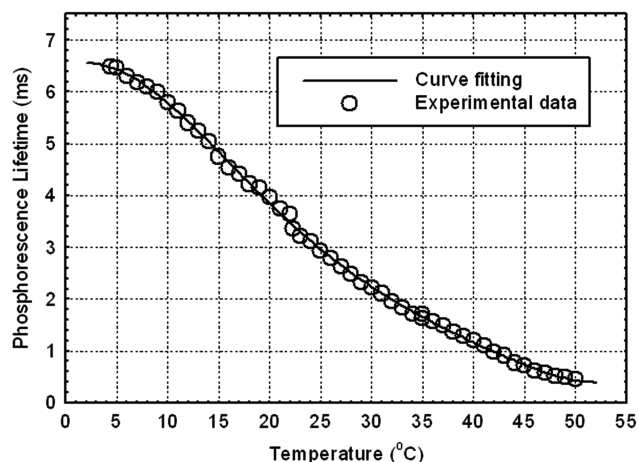


Fig. 2 Phosphorescence lifetime of 1-BrNp · Gβ-CD · ROH vs temperature.

increasing temperature, decreasing from about 6.5 ms to 0.4 ms as the temperature changes from 5°C to 50°C. The relative temperature sensitivity of the phosphorescence lifetime is about 5% per degree Celsius, which is much higher than those of commonly-used fluorescent dyes. For comparison, the temperature sensitivity of Rhodamine B for LIF measurements is usually about 2% per degree Celsius [8,9].

For a given molecular tracer, such as phosphorescent triplex 1-BrNp · Mβ-CD · ROH, and a fixed  $\Delta t$  value, Eq. (4) can be used to calculate the phosphorescence lifetime of the tagged molecules on a pixel-by-pixel basis, which would result in a distribution of the phosphorescence lifetime over a two-dimensional domain. Therefore, with a calibration profile of phosphorescence lifetime vs temperature as the one shown in Fig. 2, a two-dimensional temperature distribution can be derived from a phosphorescence image pair acquired after the same excitation laser pulse.

To implement the lifetime-based MTT technique described in the present study, only one laser pulse and one dual-frame CCD camera is required for the temperature distribution measurement. Compared with the two-color LIF method [9–11], the present lifetime-based MTT technique is much easier to implement and can significantly reduce the burden on the instrumentation and experimental setup. Because fluorescence emission is short lived with an emission lifetime on the order of nanoseconds, LIF images are usually acquired when the incident laser illumination is still on; therefore, LIF images are vulnerable to the contaminations of scattered/reflected light and any fluorescence from other substances (such as from solid surfaces for surface water droplet measurements). For the lifetime-based MTT technique described here, as indicated schematically in Fig. 1, the small time delay between the illumination laser pulse and the phosphorescence image acquisition can effectively eliminate all the effects of scattered/reflected light and any fluorescence from other substances that are present in the measurement region. Furthermore, the high temperature sensitivity of the present lifetime-based MTT technique is highly favorable for the accurate measurements of small temperature differences within small water droplets.

### III. Experiments to Demonstrate the Feasibility and Implementation of the MTT Technique

In the present study, two experiments were conducted to demonstrate the feasibility and implementation of the MTT technique described earlier. First, the effectiveness of the lifetime-based MTT technique to compensate for the effect of photobleaching for the temperature measurements was demonstrated. Then, the lifetime-based MTT technique was applied to conduct simultaneous measurements of droplet size and spatially and temporally resolved temperature distribution within a convectively cooled, micro-sized water droplet over a solid surface. This served to quantify unsteady

mass and heat transfer processes within the water droplet to elucidate underlying physics to improve our understanding about micro-physical phenomena associated with various aircraft icing studies.

Figure 3 shows the schematic of the experimental setup used for the demonstration experiments. A micro-sized water droplet was placed on an aluminum test plate. Phosphorescent triplex 1-BrNp · M $\beta$ -CD · ROH was premixed within the water droplet. A laser sheet ( $\sim 200$  mm in thickness) from a pulsed Nd:YAG at a quadrupled wavelength of 266 nm was used to tag the premixed 1-BrNp · M $\beta$ -CD · ROH molecules along the middle plane of the small water droplet, as shown in Fig. 3. A 12-bit gated intensified CCD camera (PCO DiCam-Pro, Cooke Corporation) with a fast decay phosphor (P46) was used to capture the phosphorescence emission. A 10X microscopic objective (Mitsutoyo infinity-corrected, NA = 0.28, depth of field =  $3.5 \mu\text{m}$ ) was mounted in the front of the camera. The camera was operated in the dual-frame mode, where two full-frame images of phosphorescence were acquired in a quick succession after the same laser excitation pulse. The camera and the pulsed Nd:YAG lasers were connected to a workstation via a digital delay generator (BNC 555 Digital Delay-Pulse Generator), which controlled the timing of the laser illumination and the image acquisition.

Figure 4 shows a typical phosphorescence image pair of a small water droplet placed on an aluminum test plate. The first image was acquired 0.5 ms after the laser pulse and the second image at 3.5 ms

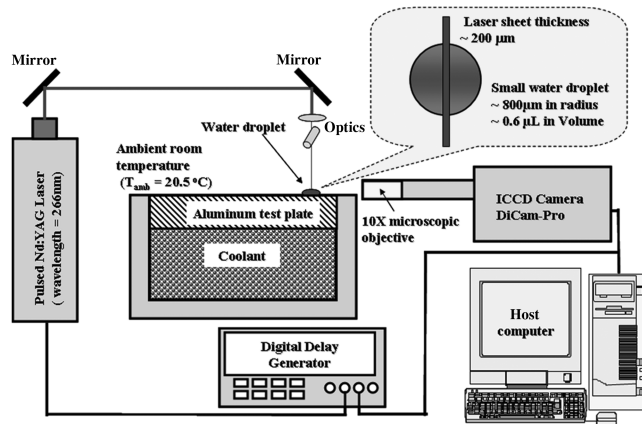
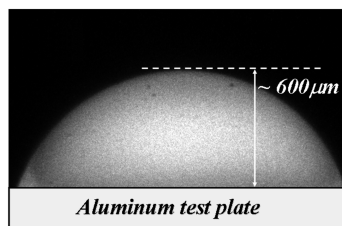
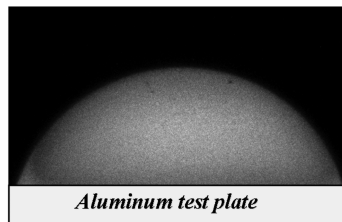


Fig. 3 Experimental setup for the demonstration experiments.



a) The first phosphorescence image acquired at 0.5 ms after laser pulse



b) The second phosphorescence image acquired at 3.5 ms after the same laser pulse

Fig. 4 A typical phosphorescence image pair acquired for MTT measurement.

after the same laser pulse with the same exposure time of 1.5 ms for the two image acquisitions. As described earlier, because the time delays between the laser excitation pulse and the phosphorescence image acquisitions can eliminate scattered/reflected light and any fluorescence from other substances (such as from a solid surface) in the measurement region effectively, the phosphorescence images of the water droplet are quite “clean.”

As described earlier, Eq. (4) can be used to calculate the phosphorescence lifetime of the tagged molecules on a pixel-by-pixel basis, which results in a distribution of the phosphorescence lifetime over a two-dimensional domain. With the calibration profile of phosphorescence lifetime vs temperature shown in Fig. 2, a two-dimensional, instantaneous temperature distribution within the water droplet can be derived from the phosphorescence image pair.

#### A. Measurement Uncertainty and Out-of-Plane Resolution

As described by Hu and Koochesfahani [3,15], the accuracy of temperature measurements attained by using the MTT technique is affected by two primary factors: 1) the image noise in the two phosphorescence images leading to noise in the estimated lifetime, and 2) potential inaccuracies in the identification of the region in the second phosphorescence image corresponding to the original tagged region in the first image.

The accuracy in the determination of lifetime from Eq. (4) and the resulting accuracy in temperature measurements are directly influenced by noise in the two phosphorescence signals  $S_1$  and  $S_2$ . For a 12-bit intensified CCD camera as that used in the present study, the actual image noise at each pixel, characterized by the standard deviation of the signal, is in the 3% range. This noise level is connected to the CCD depth of well and the intensifier stage of the CCD. As suggested by Ballew and Demas [20], the accuracy in calculating the phosphorescence lifetime can be estimated by

$$\frac{\sigma_\tau}{\tau} = \frac{1}{\ln(S_1/S_2)} \sqrt{\left(\frac{\sigma_{S_1}}{S_1}\right)^2 + \left(\frac{\sigma_{S_2}}{S_2}\right)^2} \quad (5)$$

where  $\sigma_{S_1}$ ,  $\sigma_{S_2}$ , and  $\sigma_\tau$  are the standard deviations of  $S_1$ ,  $S_2$ , and  $\tau$ , respectively. The aforementioned 3% phosphorescence signal accuracy at each pixel will, therefore, result in a lifetime measurement accuracy of about 6% and an instantaneous temperature error of  $1.2^\circ\text{C}$  (using the averaged lifetime temperature sensitivity of  $5\%$  per  $^\circ\text{C}$  for reference). Because this error is unbiased, it can be substantially reduced by averaging over neighboring pixels. Assuming statistical independence, the error can be reduced by a factor of  $1/\sqrt{N}$ , where  $N$  is the number of pixels in the interrogation window. For the results given in the present study based on a  $10 \times 10$  pixel interrogation windows, the instantaneous measurement error due to the noise in the phosphorescence images is estimated to be less than  $0.2^\circ\text{C}$ .

It should also be noted that the MTT method described here is a Lagrangian approach. The molecular region tagged in the first image convects to a new region in the second image according to its Lagrangian displacement over the time delay between the two phosphorescence image acquisitions. To determine the phosphorescence lifetime correctly, this new region in the second phosphorescence image needs to be identified.

According to Kang et al. [21], the convective Marangoni flow velocity inside an evaporating water droplet is on the order of  $10 \mu\text{m/s}$ . For the present study, the displacement of the tagged molecules due to the Marangoni flow during the time delay between the two phosphorescence image acquisitions is estimated to be about 0.02 pixels. The diffusion of the tagged tracer molecules over the time delay between the two phosphorescence image acquisitions may also result in the mismatch of the tagged tracer molecules in the two phosphorescence images. It may affect the accuracy and spatial resolution of the MTT measurements. According to Miles et al. [22], the displacement of the tagged molecules due to the molecular diffusion over the time delay between the two phosphorescence image acquisitions can be estimated to be less than 0.2 pixels for the present study.

In the present study, interrogation windows of  $10 \times 10$  pixels were used for the MTT image processing. The interrogation windows were chosen at the same locations for the first and second phosphorescence images. To assess the uncertainty level in the final measured temperature by ignoring the effects of the Marangoni flow velocity and molecular diffusion, the temperature field was computed using regions in the second phosphorescence image that were deliberately displaced an additional  $\pm 1$  pixel to exaggerate the effects of the convective Marangoni velocity and molecular diffusion. The induced mismatch resulted in a temperature error of about  $0.2^\circ\text{C}$  for the conditions of the present experiments. In addition, the procedure described here was applied to the case with a water droplet at room temperature, for which the temperature distribution within the water droplet should be uniform and constant. The measured temperature distribution within the droplet was found to have an uncertainty within  $0.5^\circ\text{C}$ . This is the total uncertainty and accounts for all the effects discussed earlier.

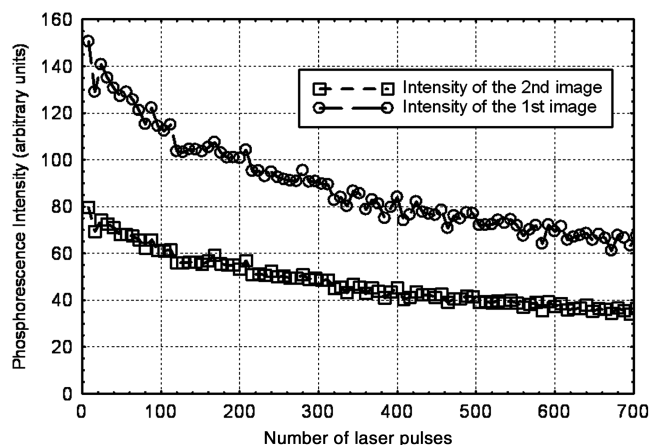
It should be noted that the laser sheet thickness used in the present study for illumination is about  $200\ \mu\text{m}$ , which is significant relative to the depth of field of the microscopic objective used for image acquisition ( $\sim 3.5\ \mu\text{m}$ ). Because all the tracer molecules within the illuminating laser sheet will be excited, the excited unfocused tracer molecules, which lie outside the focal plane of the microscopic objective, would also be detected as the background intensities in the acquired phosphorescence images. The background intensities are temperature sensitive and will contribute to the measured temperature. Therefore, the temperature measurement results given in the present study are believed to be averaged quantities over the illuminating laser sheet thickness.

## B. Measurement Results and Discussions

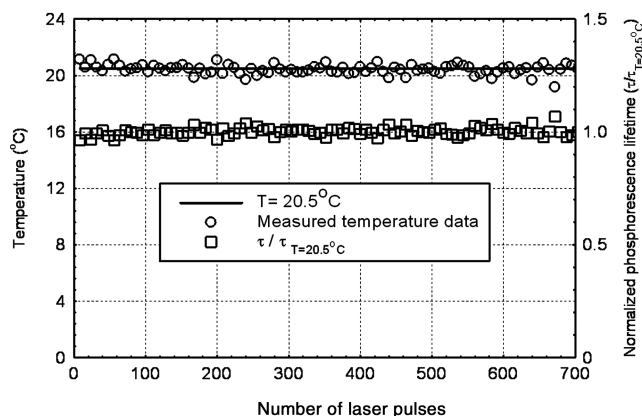
For the first demonstration experiment, no coolant was placed underneath the aluminum test plate. A micro-sized water droplet with its temperature of  $20.5^\circ\text{C}$  (room temperature) was placed on the aluminum test plate, and the surface temperature of the test plate was the same as the room temperature of  $20.5^\circ\text{C}$ , measured by using a thermocouple. Figure 5a shows the profiles of the acquired phosphorescence intensity, within a small region of  $10 \times 10$  pixels (about  $14 \times 14\ \mu\text{m}$  in a physical plane) near the center of the water droplet, for the first and second phosphorescence images as a function of the numbers of the excitation laser pulse. The acquired phosphorescence intensities were found to decay monotonically with the increasing numbers of excitation laser pulses due to the photobleaching effect. However, the calculated phosphorescence lifetime, shown in Fig. 5b, remains constant, as expected, at a level corresponding to the room temperature of  $20.5^\circ\text{C}$ . The root-mean-square value of the measured temperature was found to be about  $0.35^\circ\text{C}$ .

Then, the surface temperature of the aluminum test plate was maintained at  $2.0^\circ\text{C}$  (measured by using a thermocouple) by placing coolant underneath the aluminum test plate to demonstrate the feasibility and implementation of the lifetime-based MTT technique for simultaneous measurements of droplet size and transient temperature distribution within a convectively cooled, micro-sized water droplet on the test plate. A small water droplet ( $\sim 0.6\ \mu\text{l}$  in volume) with initial temperature of  $20.5^\circ\text{C}$  (room temperature) was placed on the aluminum test plate. The water droplet was convectively cooled after it was placed on the cold test plate.

Figure 6 shows the measured instantaneous temperature distributions within the convectively cooled water droplet as a function of the time after the droplet was placed on the test plate. As expected, the regions with lower temperature values were found to concentrate mainly near the bottom water droplet. As time went by, more and more dark regions (i.e., lower temperature regions) were found in the measured instantaneous temperature distributions, which indicates that the temperature of the water droplets became lower and lower due to the convective cooling. It should also be noted that rather noisy structures of the temperature contour lines can be found from the instantaneous temperature distributions. Given the present level of the measurement uncertainty and the small



a) Acquired phosphorescence intensities vs. number of laser pulse



b) Derived phosphorescence lifetime and temperature vs. numbers of laser pulse

Fig. 5 Compensation of the photobleaching effect.

temperature variation within the small water droplet, it is still quite difficult to conclude whether the noisy structures in the measured instantaneous temperature distributions are physical or mainly due to the measurement error. Further work is needed to clarify the ambiguities.

Figure 7 shows the profile of the spatially averaged temperature of the water droplet as a function of time, which was calculated based on the time sequence of the measured instantaneous temperature distributions. The characteristics of the unsteady heat transfer process within the convectively cooled water droplets were revealed quantitatively from the evolution of the spatially averaged temperature of the water droplet. Because the initial temperature of the water droplet ( $20.5^\circ\text{C}$ ) was significantly higher than that of the cold aluminum test plate ( $2^\circ\text{C}$ ), the spatially averaged temperature of the water droplet was found to decrease rapidly and monotonically after it was placed on the cold aluminum test plate. The temperature measurement results given in Fig. 7 also revealed that a thermal steady state would be reached at about 150 s later, after the water droplet was placed on the cold test plate. The spatially averaged temperature of the water droplet would not decrease anymore when the thermal steady state was reached. The spatially averaged temperature of the water droplet was found to be about  $6^\circ\text{C}$  after the thermal steady state was reached.

In addition to the transient temperature distribution measurements within the small water droplet, the size (in terms of volume, height, contact area, and contact angle) of the water droplet on the test plate can also be determined simultaneously from the acquired phosphorescence images with a predetermined scale ratio between the image plane and objective plane. Therefore, the characteristics of the unsteady mass process of the water droplet on the aluminum test

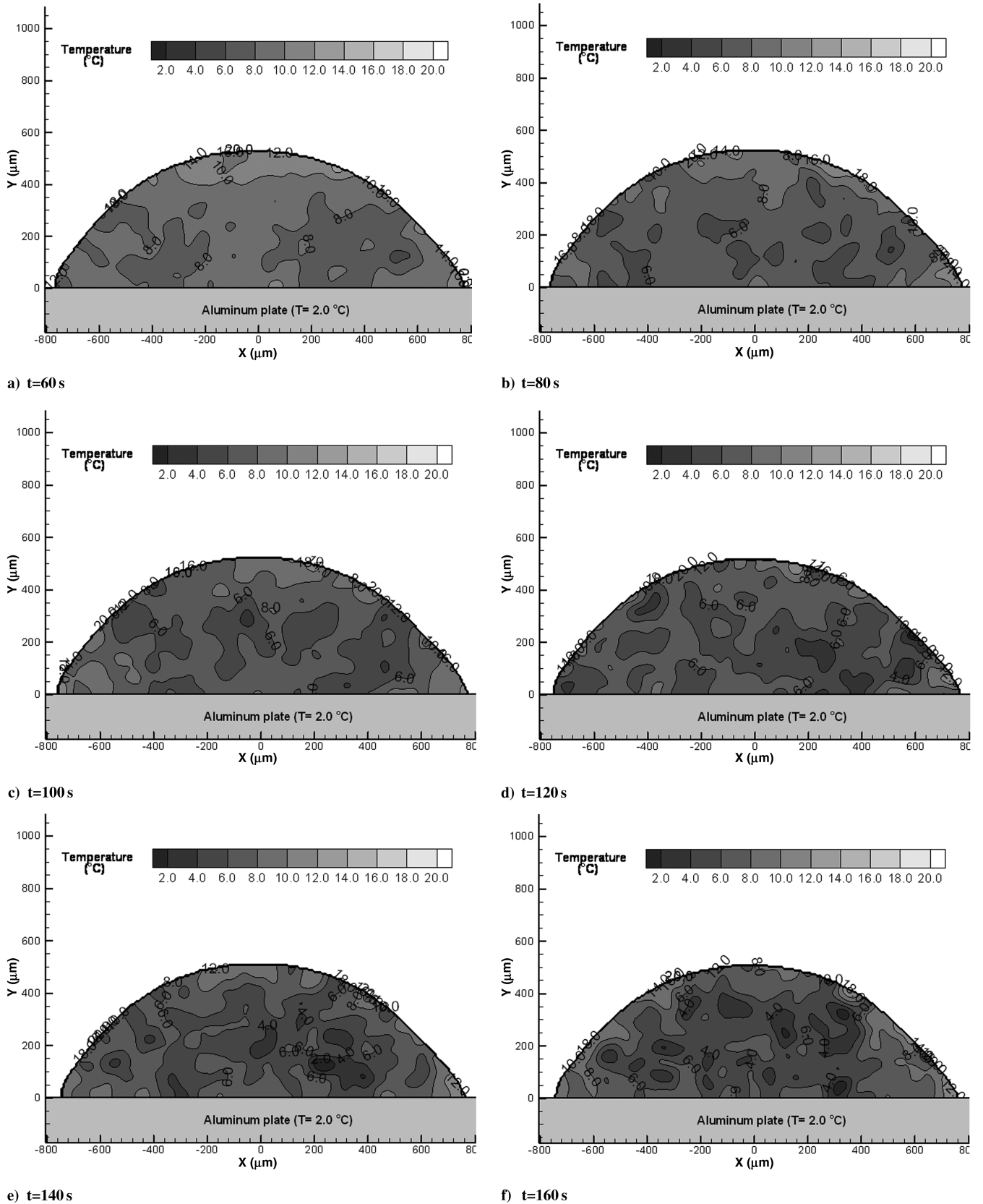


Fig. 6 Instantaneous temperature distributions within the convectively cooled water droplet.

plate due to evaporation can also be quantified from the MTT measurement results.

Figure 8 shows schematically the definitions of water droplet height  $H$ , contact radius  $R$ , contact angle  $\theta$ , and volume  $V$  used in the present study. As shown in Fig. 4, the edge of the water droplet can be

easily detected based on the significant intensity changes in the acquired phosphorescence images. Thus, the contact radius  $R$  and droplet height  $H$  can be measured directly from the acquired phosphorescence images with a predetermined scale ratio between the image plane and objective plane. The contact angle  $\theta$  and volume

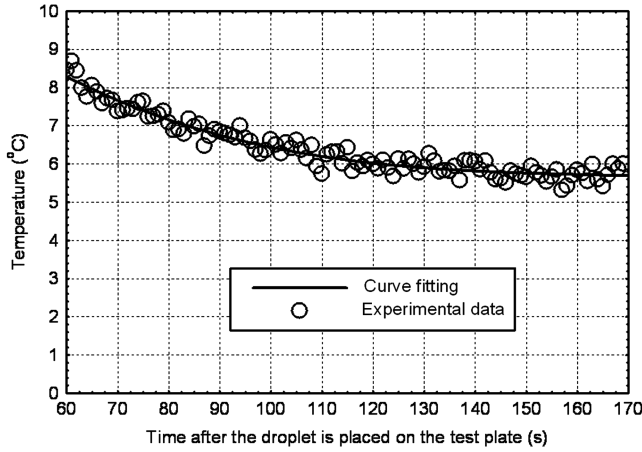


Fig. 7 Spatially averaged temperature of a small water droplet vs time.

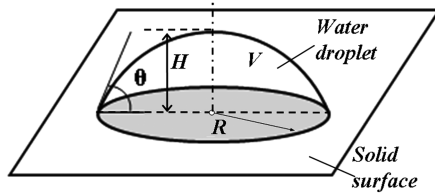


Fig. 8 Schematic of a surface water droplet.

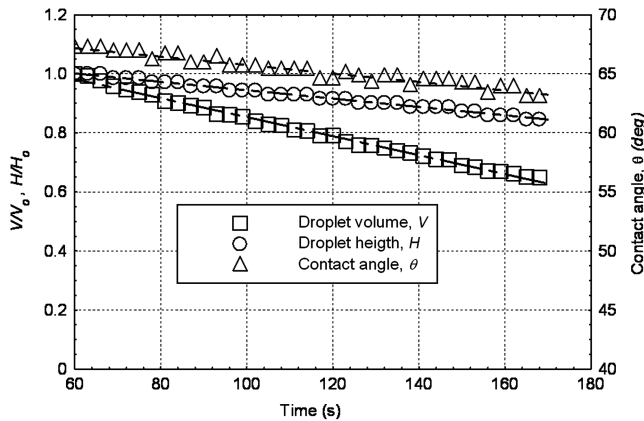


Fig. 9 Evolution of volume, height, and contact angle of the water droplet due to evaporation.

$V$  were determined by using the following equations based on the fact that a surface droplet is normally a sphere cap:

$$\theta = 2\arctan\left(\frac{H}{R}\right) \quad (6)$$

$$V = \frac{\pi R^3 (1 - \cos \theta)^2 (2 + \cos \theta)}{3 \sin^3 \theta} \quad (7)$$

It is well known that there are two modes for the evaporation of a liquid droplet on a solid surface [23–25]; one consists of a constant contact angle with diminishing contact area and the other consists of a constant contact-area with a diminishing contact angle. The phosphorescence image pair given in Fig. 4 visualizes clearly that the contact angle of the water droplet on the aluminum test plate was less than 90 deg. The radius of the contact area of the water droplet on the aluminum test plate was found to be almost constant during the experiments, which indicates that the evaporation process of the

water droplet followed the constant contact-area mode. Figure 9 shows the measured water droplet size (in the terms of droplet volume, height, and contact angle) on the aluminum test plate as a function of time after it was placed on the test plate. It can be seen clearly that the droplet height, volume, and contact angle decreased linearly with time due the evaporation. The results were found to agree with the findings of Birdi et al. [25], who suggested that for a liquid drop on a low-surface-tension solid surface, the evaporation rate would be linear and follow the constant contact-area mode if the initial contact angle of the droplet is less than 90 deg.

As demonstrated by the measurement results shown earlier, the lifetime-based MTT technique described in the present study is capable of providing detailed measurements to quantify the unsteady mass and heat transfer processes within convectively cooled, small water droplets on solid surfaces. Such information is highly desirable to elucidate underlying physics to improve our understanding about microphysical phenomena for various aircraft icing studies.

#### IV. Conclusions

In the present study, a lifetime-based molecular tagging thermometry technique was developed and implemented to achieve simultaneous measurements of droplet size (in terms of volume, height, contact-area, and the contact angle of the water droplet) and temporally and spatially resolved temperature distributions within micro-sized water droplets on solid surfaces. Unlike most commonly used LIF-based techniques that rely on information obtained from the intensity axis of the fluorescence emission process, the lifetime-based MTT technique described in the present study relies on the information contained in the time axis of the phosphorescence emission process, as temperature change would cause significant variations in the phosphorescence lifetime of some phosphorescent dyes.

Water-soluble phosphorescent triplex  $1\text{-BrNp} \cdot \text{M}\beta\text{-CD} \cdot \text{ROH}$  was used in the present study as the molecular tracer for the simultaneous droplet size and transient temperature distribution measurements within small water droplets. A pulsed laser is used to tag the phosphorescent triplex  $1\text{-BrNp} \cdot \text{M}\beta\text{-CD} \cdot \text{ROH}$  molecules premixed within a small water droplet. Long-lived laser-induced phosphorescence emitted from the tagged tracer molecules is imaged at two successive times after the same laser excitation pulse. While the size of the water droplet is determined from the acquired phosphorescence images with a predetermined scale ratio between the image plane and objective plane, the temperature measurement is achieved by taking advantage of the temperature dependence of phosphorescence lifetime, which is estimated from the intensity ratio of the acquired phosphorescence image pair.

The implementation and application of the lifetime-based MTT technique were demonstrated by conducting simultaneous measurements of droplet size and temporally and spatially resolved temperature distribution within a small, convectively cooled water droplet ( $\sim 0.6 \mu\text{l}$  in volume) placed on an aluminum test plate to quantify unsteady mass and heat transfer processes within the small water droplet. Dynamic change of the temperature distribution within the micro-sized water droplets in the course of the convective cooling process were quantified clearly from the MTT measurement results. Time evolution of the size change of the small water droplet (in terms of volume, height, contact-area, and the contact angle of the water droplet) due to evaporation was also revealed quantitatively. Such information is highly desirable to elucidate underlying physics to improve our understanding about microphysical phenomena associate with aircraft icing studies.

#### Acknowledgments

The support of National Science Foundation CAREER program under award number of CTS-0545918 is gratefully acknowledged. The authors also want to thank Manoochehr Koochesfahani of Michigan State University for providing the optical lenses and chemicals used for the present study.

## References

- [1] Gent, R. W., Dart, N. P., and Cansdale, J. T., "Aircraft Icing," *Philosophical Transactions. Series A, Mathematical, Physical, and Engineering Sciences*, Vol. 358, No. 1776, 2000, pp. 2873–2911. doi:10.1098/rsta.2000.0689
- [2] "Aircraft Accident Report: In-flight Icing Encounter and Loss of Control Simmons Airlines, d.b.a. American Eagle Flight 4184," Report NTSB/AAR-96/01, PB96-910401, Vol. 1, July 1996.
- [3] Hu, H., and Koochesfahani, M., "Molecular Tagging Velocimetry and Thermometry and its Application to the Wake of a Heated Circular Cylinder," *Measurement Science and Technology*, Vol. 17, No. 6, 2006, pp. 1269–1281. doi:10.1088/0957-0233/17/6/S06
- [4] Pringsheim, P., *Fluorescence and Phosphorescence*, Interscience, New York, 1949.
- [5] Lu, Q., and Melton, A., "Measurement of Transient Temperature Field Within a Falling Droplet," *AIAA Journal*, Vol. 38, No. 1, 2000, pp. 95–101. doi:10.2514/2.927
- [6] Lavielle, P., Lemoine, F., Lavergne, G., and Lebouche, M., "Evaporating and Combusting Droplet Temperature Measurements Using Two-Color Laser-Induced Fluorescence," *Experiments in Fluids*, Vol. 31, No. 1, 2001, pp. 45–55. doi:10.1007/s003480000257
- [7] Harris, S. R., Lempert, W. R., Hersh, L., Burcham, C. L., Saville, D. A., Miles, R. B., Gee, K., and Haughland, R. P., "Quantitative Measurements of Internal Circulation in Droplets Using Flow Tagging Velocimetry," *AIAA Journal*, Vol. 34, No. 3, 1996, pp. 449–454. doi:10.2514/3.13088
- [8] Coppeta, J., and Rogers, C., "Dual Emission Laser Induced Fluorescence for Direct Planar Scalar Behavior Measurements," *Experiments in Fluids*, Vol. 25, No. 1, 1998, pp. 1–15. doi:10.1007/s003480050202
- [9] Sakakibara, J., and Adrian, R. J., "Whole Field Measurement of Temperature in Water Using Two-Color Laser Induced Fluorescence," *Experiments in Fluids*, Vol. 26, No. 1, 1999, pp. 7–15. doi:10.1007/s003480050260
- [10] Escobar, S., Gonzalez, J. E., and Rivera, L. A., "Laser-Induced Fluorescence Temperature Sensor for In-Flight Droplet," *Experimental Heat Transfer*, Vol. 14, No. 2, 2001, pp. 119–134.
- [11] Wolff, M., Delconte, A., Schmidt, F., Gucher, P., and Lemoine, F., "High-Pressure Diesel Spray Temperature Measurements Using Two-Color Laser Induced Fluorescence," *Measurement Science and Technology*, Vol. 18, No. 3, 2007, pp. 697–706. doi:10.1088/0957-0233/18/3/020
- [12] Omrane, A., Juhlin, G., Ossler, F., and Alden, M., "Temperature measurements of single droplets by use of laser-induced phosphorescence," *Applied Optics*, Vol. 43, No. 17, 2004, pp. 3523–3529. doi:10.1364/AO.43.003523
- [13] Omrane, A., Santesson, S., Alden, M., and Nilsson, S., "Laser Techniques in Acoustically Levitated Micro Droplets," *Lab on a Chip*, Vol. 4, No. 4, 2004, pp. 287–291. doi:10.1039/b402440k
- [14] Hu, H., Lum, C., and Koochesfahani, M., "Molecular Tagging Thermometry with Adjustable Temperature Sensitivity," *Experiments in Fluids*, Vol. 40, No. 5, 2006, pp. 753–763. doi:10.1007/s00348-006-0112-2
- [15] Hu, H., and Koochesfahani, M., "A Novel Technique for Quantitative Temperature Mapping in Liquid by Measuring the Lifetime of Laser Induced Phosphorescence," *Journal of Visualization*, Vol. 6, No. 2, 2003, pp. 143–153.
- [16] Ponce, A., Wong, P. A., Way, J. J., and Nocera, D. G., "Intense Phosphorescence Triggered by Alcohol upon Formation of a Cyclodextrin Ternary Complex," *Journal of Physical Chemistry*, Vol. 97, No. 42, 1993, pp. 11137–11142. doi:10.1021/j100144a040
- [17] Hartmann, W. K., Gray, M. H. B., Ponce, A., and Nocera, D. G., "Substrate Induced Phosphorescence from Cyclodextrin-Lumophore Host-Guest Complex," *Inorganica Chimica Acta*, Vol. 243, No. 1, 1996, pp. 239–248.
- [18] Gendrich, C. P., and Koochesfahani, M. M., "A Spatial Correlation Technique for Estimating Velocity Fields Using Molecular Tagging Velocimetry (MTV)," *Experiments in Fluids*, Vol. 22, No. 1, 1996, pp. 67–77. doi:10.1007/BF01893307
- [19] Koochesfahani, M. M., and Nocera, D. G., "Molecular Tagging Velocimetry," *Handbook of Experimental Fluid Dynamics*, edited by J. Foss, C. Tropea, and A. Yarin, Springer-Verlag, Berlin, 2007, Chap. 5.4.
- [20] Ballew, R. M., and Demas, J. N., "An Error Analysis of the Rapid Lifetime Determination Method for the Evaluation of Single Exponential Decay," *Analytical Chemistry*, Vol. 61, No. 1, 1989, pp. 30–33. doi:10.1021/ac00176a007
- [21] Kang, K. H., Lee, S. J., Lee, C. M., and Kang, I. S., "Quantitative Visualization of Flow Inside an Evaporating Droplet Using the Ray Tracing Method," *Measurement Science and Technology*, Vol. 15, No. 6, 2004, pp. 1104–1112. doi:10.1088/0957-0233/15/6/009
- [22] Miles, R. B., Grinstead, J., Kohl, R. H., and Diskin, G., "The RELIEF Flow Tagging Technique and its Application in Engine Testing Facilities and for Helium-Air Mixing Studies," *Measurement Science and Technology*, Vol. 11, No. 9, 2000, pp. 1272–1281. doi:10.1088/0957-0233/11/9/304
- [23] Picknett, R. G., and Bexon, R., "The Evaporation of Sessile or Pendant Drops in Still Air," *Journal of Colloid and Interface Science*, Vol. 61, No. 2, 1977, pp. 336–350. doi:10.1016/0021-9797(77)90396-4
- [24] Rowan, S. M., Newton, M. I., and McHale, G., "Evaporation of Microdroplets and the Wetting of Solid Surfaces," *Journal of Physical Chemistry*, Vol. 99, No. 35, 1995, pp. 13268–13271. doi:10.1021/j100035a034
- [25] Birdi, K. S., Vu, D. T., and Winter, A., "A Study of the Evaporation Rates of Small Water Drops Placed on Solid," *Journal of Physical Chemistry*, Vol. 93, No. 9, 1989, pp. 3702–3703. doi:10.1021/j100346a065

A. Naguib  
Associate Editor